THE JOURNAL OF PHYSICAL CHEMISTRY A

ARTICLE

pubs.acs.org/JPCA

Ultrafast Forward and Backward Electron Transfer Dynamics of Coumarin 337 in Hydrogen-Bonded Anilines As Studied with Femtosecond UV-Pump/IR-Probe Spectroscopy

Hirendra N. Ghosh,*[,†,‡] Sandeep Verma,[†] and Erik T. J. Nibbering*[,‡]

[†]Radiation & Photochemistry Division, Bhabha Atomic Research Centre, Trombay Mumbai −400085, India

[‡]Max Born Institute for Nonlinear Optics and Short Pulse Spectroscopy, Max Born Strasse 2A, D-12489, Berlin, Germany

Supporting Information

ABSTRACT: Femtosecond infrared spectroscopy is used to study both forward and backward electron transfer (ET) dynamics between coumarin 337 (C337) and the aromatic amine solvents aniline (AN), *N*-methylaniline (MAN), and *N*,*N*-dimethylaniline (DMAN), where all the aniline solvents can donate an electron but only AN and MAN can form hydrogen bonds with C337. The formation of a hydrogen bond with AN and MAN is confirmed with steady state FT-IR spectroscopy, where the C═O stretching vibration is a direct marker mode for hydrogen bond formation. Transient IR absorption measurements in all solvents show an absorption band at 2166 cm^{-1}, which has been attributed to the C≡N stretching vibration of the C337 radical anion formed after ET. Forward electron transfer dynamics is found to be biexponential with time constants $\tau_{ET}{}^{1}$ = 500 fs, $\tau_{ET}{}^{2}$ = 7 ps in all solvents. Despite the presence of hydrogen bonds of C337 with the solvents AN and MAN, no effect has been found on the forward electron transfer step. Because of the absence of an H/D isotope effect on the forward electron transfer reaction of C337 in AN, hydrogen bonds are understood to play a minor role in mediating electron transfer. In contrast, direct π-orbital overlap between C337 and the aromatic amine solvents causes ultrafast forward electron transfer dynamics. Backward electron transfer dynamics, in contrast, is dependent on the solvent used. Standard Marcus theory explains the observed backward electron transfer rates.

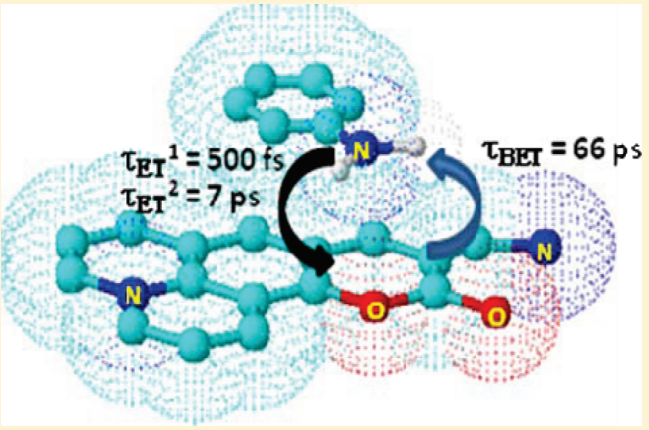

1. INTRODUCTION

Considerable progress in both theory and experiment has been witnessed in the last few decades in the field of electron transfer (ET) dynamics.[1] Photoinduced electron transfer (ET) reactions between donor and acceptor moieties are ubiquitous in light harvesting and solar energy conversion[2] and biological systems.[3] The dynamical time scales of ET and the associated efficiencies are governed by electronic coupling between donor and acceptor. Underlying mechanisms for such ET reactions include through space couplings, and through bond couplings, that can either be of covalent nature or consist of hydrogen bonds or involve $\pi-\pi$ orbital overlap linking donor and acceptor units.[4] Whereas through space couplings usually involve a large range of spatial degrees of freedom, couplings through chemical bonds possess a high degree of directionality. Hydrogen bonds control the separation distance and relative orientation between donor and acceptor.[5] In the case of ET in proteins and DNA, electronic coupling is thus strongly affected by the hydrogen bond networks making up the three-dimensional structure of those biological systems.[6] Moreover, several studies have demonstrated that hydrogen bonds can mediate electron transfer efficiently.[7] As such it has generally been recognized that the function of hydrogen bonds in biological systems most likely extends beyond simply providing the structural scaffolding for the donors and acceptors which participate in the redox process. However, whether hydrogen bonds play the most dominating role in ET remains a topic for continuous study, as every ET process between donor and acceptor units may also be controlled by solvent reorganization or other types of donor−acceptor interactions such as $\pi-\pi$ orbital overlap.

Photoinduced bimolecular ET between donor and acceptor molecules in liquid solution has been a widely studied topic[8−10] Time-resolved studies have, until now, mostly focused on the forward ET transfer after photoexcitation of either donor or

Received: August 26, 2010
Revised: November 2, 2010
Published: December 30, 2010

acceptor molecules. Many of these studies have relied on time-resolved fluorescence techniques, revealing the electronic excited state decay of the chromophore after photoinitiation, caused by oxidative ET with an acceptor molecule[8] or by reductive ET from a donor molecule.[9,10] Time-resolved UV/vis pump−probe spectroscopy of electronic transitions of the donor and acceptor molecules and of the radical cations and anions formed upon ET, on the other hand, may in principle provide insight in both forward and backward ET dynamics. This approach is, however, strongly hampered by the extreme broadening typical for electronic transitions, and as such structural information on the ET process has remained limited.[11] In contrast, transient vibrational spectroscopy may provide more in-depth information on the geometry of donor−acceptor reaction pairs, as has recently been obtained on the photoinduced oxidative ET between $\pi-\pi$ stacked perylene−tetracyanoethene molecules.[10] Until now, however, such an approach has not been applied to photoinduced ET between donor and acceptor species where hydrogen bond dynamics could be playing a major role.

We present here femtosecond infrared spectroscopic results on the photoinduced reductive ET of a coumarin dye and aromatic amine solvents. Yoshihara and co-workers reported on ultrafast electron transfer dynamics in photoexcited acceptor coumarin dyes dissolved in donating aromatic amines. Here a collection of coumarin dyes were used, to explore ET driving force dependencies, and the aromatic family of anilines with different substituents on the amino group, including the solvents aniline (AN), *N*-methylaniline (NMAN), and *N*,*N*-dimethylaniline (DMAN), to investigate the effects of hydrogen bonding dynamics. Hydrogen bonding is expected to occur between the hydrogen bond donating groups of AN and NMAN and the C═O moiety of the coumarin dyes, whereas this is not possible with DMAN. Because in most of these studies the fluorescence upconversion technique was used, information has been obtained only on the forward ET process. In the forward ET reaction between these coumarin dyes and the aromatic amine solvents, only a minor H/D isotope effect has been found, suggesting that ET is not strongly mediated by any possible site-specific solute−solvent hydrogen bonding. Instead, with ET reaction rates for the investigated systems often faster than solvation dynamics, electronic couplings appear to play a more important role dictating the ET dynamics.

Ultrafast IR spectroscopy provides key insight into the dynamics of site-specific hydrogen bond interactions between solute and solvent affected by electronic excitation, as has been demonstrated by Chudoba et al.[12] on coumarin 102 (C102) dissolved in chloroform or hydrogen bonded with methanol in nonpolar solvent. Palit et al.[13] used this approach to investigate the hydrogen bond dynamics of C102 in the electronic excited state in AN solvent. C102−AN, however, does not exhibit an ultrafast electron transfer reaction. Recently, using time-dependent density functional theory, Liu et al. calculated that the intermolecular C102−AN hydrogen bond, connecting the C═O group of C102 and the NH of the amino group of AN, is significantly strengthened upon electronic excitation.[14] Wang et al.[11] reported on the ultrafast forward electron transfer dynamics between coumarin 337 (C337) and DMAN solvent using a combined ultrafast UV/IR and UV/vis spectroscopic approach. Whereas a forward ET rate with a 4 ps time constant was reported, no details were given on the backward ET process, and in addition no hydrogen bonding effects using other aniline solvents were explored.

Scheme 1. Molecular Structures of C337 (Acceptor) and *N*-Methylated Anilines (Donors)

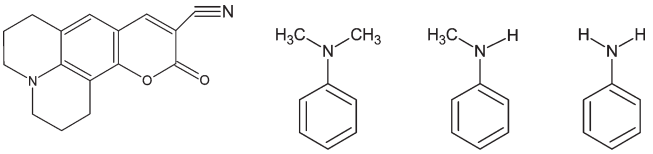

C337 DMAN NMAN AN

We now present results on C337 dissolved in AN, NMAN, and DMAN (Scheme 1). We have carried out femtosecond UV-pump/IR-probe measurements of C337 dissolved in these aromatic amine solvents by exciting C337 to the S_1-state using pump pulses tuned at 400 nm and probing absorbance changes of vibrational marker bands. Using this approach we can determine both forward and backward electron transfer rates. Whereas effects of hydrogen bonds turn out to be of minor magnitude, we conclude that other electronic coupling mechanisms, in particular stacking of the π-orbitals of C337 and the aromatic solvents, play a more important role.

2. EXPERIMENTAL SECTION

To follow the temporal evolution of vibrational marker modes, we used a femtosecond infrared spectroscopic laser system consisting of a 1 kHz amplified Ti:sapphire regenerative and booster amplifier system (Spitfire Pro, Spectra Physics) and frequency conversion stages. The second harmonic output of the amplified laser system (wavelength 400 nm, pulse duration 55 fs, energy 3−7 μJ, spot diameter 300 λm) was used to excite C337. Tunable mid-IR probe pulses (100−150 fs duration, 10 nJ energy) were generated by difference frequency mixing of signal and idler pulses from a near-infrared optical parametric amplifier.[15] Probe and reference pulses were derived using reflections from a BaF_2 wedge and focused onto the sample with off-axis parabolic mirrors (focal diameter 100 mm). After spectral dispersion with a polychromator, the probe pulses were detected by a multichannel mid-IR detector array (IR associates) with a spectral resolution of 4−8 cm^{-1}, depending on the spectral region probed. The whole pump−probe setup was purged with nitrogen gas to avoid spectral and temporal reshaping of the mid-IR pulses by the absorption of water vapor and CO_2 in air. For reference purposes the sample was replaced by a polished ZnSe window to determine the zero delay point (including the chirp of the IR pulse) and to control the time resolution of the cross-correlation (fwhm 120−140 fs). The relative polarization of the pump and probe pulses were set under magic angle to detect ET dynamics not affected by rotational diffusion effects.

Sample solutions were circulated through a flow cell consisting of 1 mm thick BaF_2 windows separated by a 100 μm thick Teflon spacer, to guarantee that for every laser shot a new fraction of the solution was excited. We used 10 mM solutions of C337 (Aldrich) in the femtosecond pump−probe experiments. Aniline (AN), *N*-methylaniline (NMAN), and dimethylaniline (DMAN) were obtained from Fluka. Deuterated aniline-d_2, $C_6H_5ND_2$, was obtained by H/D exchange using D_2O (Deutero GmbH), followed by extraction of the organic phase and further drying. All measurements were performed at room temperature, T = 25 ± 2 °C.

dx.doi.org/10.1021/jp108090b |*J. Phys. Chem. A* 2011, 115, 664–670

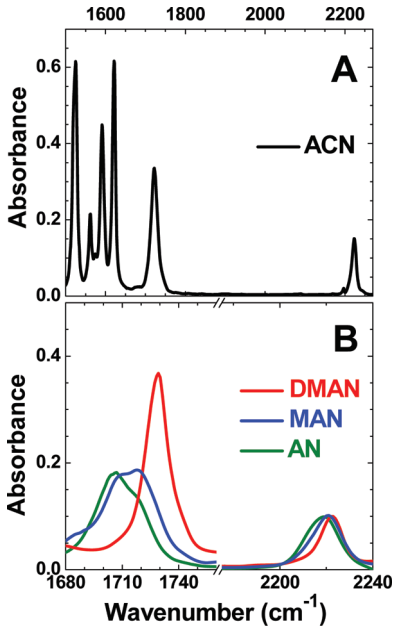

Figure 1. Panel A: Ground state infrared spectrum of C337 in acetonitrile (ACN). The infrared absorption at 1500−1650 cm^{-1} can be attributed to the stretching mode C═C ring vibration, the band in the 1690−1740 cm^{-1} region to the stretching mode of the C═O group, and the band in the 2220−2250 cm^{-1} region to the stretching mode of the C≡N vibration. Panel B: Steady state IR spectra of C337 in AN, MAN, and DMAN from 1680 to 2240 cm^{-1} showing only the C═O and C≡N stretching modes.

3. EXPERIMENTAL RESULTS

3.1. Steady-State IR Spectra of C337. Panel A of Figure 1 shows the FT-IR spectra of C337 in acetonitrile. The bands in the 1500−1650 cm^{-1} region can be attributed to C═C ring vibrational modes. The sharp band located at 1722 cm^{-1} is the C═O stretching vibrational transition of C337. The C≡N marker mode has its transitional frequency at 2223 cm^{-1}. This provides us with at least two distinct marker modes, the C═O and C≡N vibrations, with which we can probe the photoinduced ET reaction. Hydrogen bonding with protic solvents is expected to occur at the C═O group of C337 (panel B, Figure 1). Indeed, when dissolving C337 in AN, MAN, and DMAN, the frequency position of the C═O marker mode clearly exhibits a red-shift in AN and to a lesser extent in MAN, whereas in DMAN the C═O stretching band is located at the same position as in other non-hydrogen bonding solvents (panel A, Figure 1). The two-peaked structure of the C═O stretching mode in MAN (1718 and 1709 cm^{-1}) and in AN (1717 and 1706 cm^{-1}) could be assigned to a non-hydrogen-bonded C337 and a C337-solvent hydrogen-bonded complex, respectively, or to a Fermi resonance splitting (often observed for coumarin dyes) of the C═O stretching band of C337 hydrogen bonded to the solvent. Indeed, a small solvent shift due to changes in dielectric constant of the solvent when going from DMAN to MAN or AN may occur without having a hydrogen bond at the C═O moiety. Another possibility is the interaction between the π-orbitals of C337 and nearby aromatic amine solvent molecules that may be larger for AN and less so for DMAN due to steric hindrance of the double-alkylated amino group. Minor frequency shifts also happen in the case of the C≡N stretching band, where hydrogen bonds with the solvent are not expected to directly occur at this functional group. We find that the C≡N band is located at 2222, 2220, and 2218 cm^{-1} for DMAN, NMAN, and AN, respectively. Such small shifts may be caused by dielectric constant changes, or by the indirect effect of hydrogen bonds when an aromatic amine solvent molecule complexes with the C═O group, or when $\pi-\pi$ stacking occurs between C337 and the aromatic amine solvent molecules. The spectral width of the C≡N transition also increases slightly when going from DMAN, via NMAN, to AN as solvent. One can conclude from these steady FT-IR spectra that C337 has a stronger interaction with the solvent molecules when going from DMAN, via MAN, to AN, likely caused by a direct coupling between the electrical dipoles of C337 and the solvent and/or $\pi-\pi$ stacking between the aromatic π-orbitals, accompanied by an increasing hydrogen bond strength with an additional solvent molecule at the C═O group.

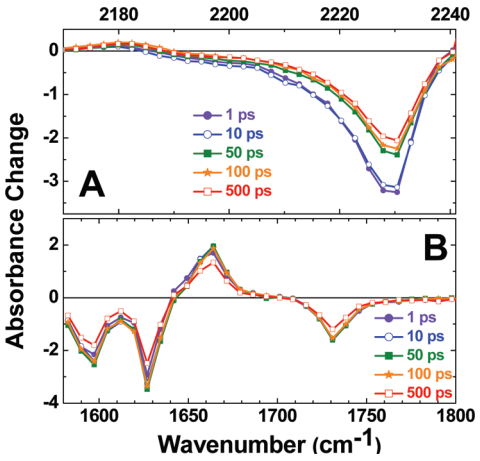

Figure 2. Transient IR absorption spectra of C337 in acetonitrile at different time delays after excitation at 400 nm. Panel A shows the C≡N stretching region. Panel B depicts the upper part of the fingerprint region.

3.2. Transient IR Absorption Spectroscopy of C337 in Acetonitrile. We first present transient IR results of C337 in the non-hydrogen bonding and nonreacting solvent acetonitrile (ACN). Panel B of Figure 2 shows the transient IR absorption spectra of C337 in the spectral region from 1580 to 1800 cm^{-1} recorded at several pulse delays after exciting with the 400 nm pump pulse. The transient spectra show the time-resolution limited generation of bleach signals at 1597, 1626, and 1737 cm^{-1}, directly correlated with the peak positions of C═C and C═O stretching signals of C337 in the electronic ground state. In addition to these bleach signals, a positive absorption band at 1664 cm^{-1} appears within temporal resolution, which we assign as the C═O stretching vibration of C337 in the first electronic excited state. This band decays on a time scale >1 ns (beyond the maximum scanning range of our delay stage), in accordance with bleach recovery with a similar time constant, suggesting an S_1-state lifetime larger than 1 ns. We have determined the electronic excited state lifetime using time-correlated single photon counting of the fluorescence emission to be 3.7 ns (see Supporting Information, Figure S3). We have also carried out transient absorption studies of the C≡N stretching frequency region from 2160 to 2240 cm^{-1} (panel A, Figure 2). The transient spectra show a clear bleach signal at 2230 cm^{-1} indicative of the C≡N stretching mode of C337 in the S_0-state. We have identified a positive signal located at 2180 cm^{-1} and attribute this to the C≡N stretching mode of C337 in the S_1-state. We note that

dx.doi.org/10.1021/jp108090b |J. Phys. Chem. A 2011, 115, 664–670

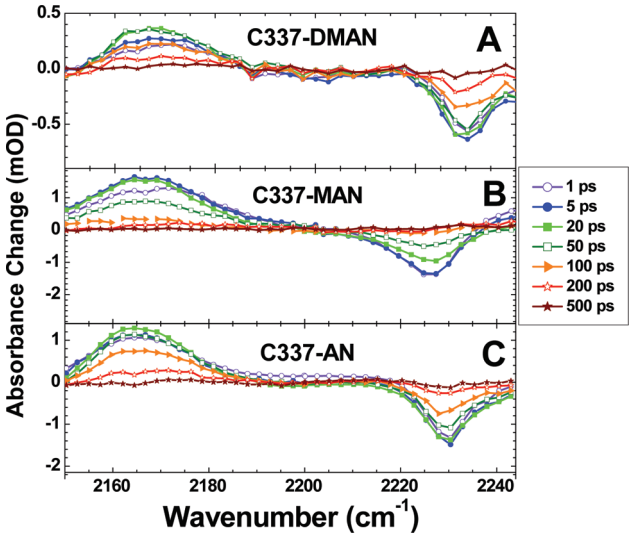

Figure 3. Transient IR absorption spectra of C337 in different amine solvents as function of time delay after excitation at 400 nm. Panel A: in DMAN. Panel B: in MAN. Panel C: in AN.

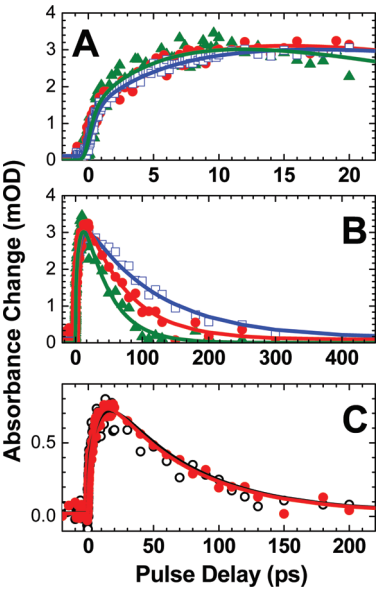

Figure 4. Transient population kinetics at 2166 cm^{-1} of C-337 in AN (red filled dots), MAN (green filled triangles), and DMAN (open blue squares). Panel A: Early time population kinetics, showing the forward ET dynamics. Panel B: Long time population kinetics, showing the solvent dependent back ET dynamics. Panel C: Comparison of the population kinetics in AN-h_2 and AN-d_2, showing the absence of H/D isotope effects on the forward and backward ET dynamics in aniline.

upon electronic excitation of C337 this C≡N stretching vibration has, besides its frequency downshift of 50 cm^{-1}, a significant decrease in oscillator strength compared to its value in the S_0-state, in strong contrast to the C═O stretching vibration which shows merely a frequency downshift of 73 cm^{-1} without much change in oscillator strength. The fact that both bands downshift in frequency provides insight into the charge redistribution upon excitation to the S_1-state.

3.3. Transient IR Absorption of C337 in Aromatic Amine Solvents. The aromatic amine solvents have a pronounced steady state absorption in the spectral range of the C═O stretching vibration, preventing probing this important marker mode when exciting C337 in these solvents. We thus have to rely on the transient response of the C≡N marker band to learn about the ET dynamics. Figure 3 shows the transient IR spectra of C337 in DMAN, MAN, and AN, recorded in the C≡N stretching region. Apart from the bleach signal located at the C≡N stretching transition frequency of C337 in the S_0-state, we observe a positive transient signal at 2166 cm^{-1}. Such a frequency shift is significantly larger than the frequency shift we have recorded of the C≡N stretching vibration of C337 when going from the S_0-state to the S_1-state. Moreover, now this positive signal has about similar magnitude as the bleach signal at 2230 cm^{-1}. Whereas the bleach appears within temporal resolution, and recovers with a time constant of 110 ps in DMAN, the positive band at 2166 cm^{-1} grows in a nonexponential fashion on picosecond time scales and decays with the same 110 ps time constant as the bleach recovers (Figure 4A, B). The decay of the positive signal and the bleach recovery are for all solvents identical, however with a varying solvent dependent time constant: we measure it to be 40 ps in MAN and 66 ps in AN. The nonexponential rise can be fitted with a biexponential function, using in contrast the same time constants for all solvents: τ_1= 500 fs and τ_2=7 ps, where now the relative magnitudes weakly depend on the electron donating solvent used: A_1 = 33% and A_2 = 67% for DMAN, A_1 = 27% and A_2 = 73% for MAN, and A_1 = 23% and A_2=77% for AN. We have in addition performed an experiment using AN-d_2 and found no isotope effect on the rise of the 2166 cm^{-1} band, and only a small difference on the decay of the band (Figure 4C).

4. DISCUSSION

Based on the fact that in the aromatic amine solvents the S_1-state of C337 is short-lived, converting via an intermediate state with a C≡N stretching vibration located at a different frequency position back to the electronic ground state, we conclude that upon photoexcitation of C337 reductive forward electron transfer from the electron donating amine solvents occurs, generating a $C337^{\bullet-}$ radical anion and the aromatic amine radical cation. This ion pair then follows the backward electron transfer reaction pathway recovering C337 in the electron ground state and neutral solvent molecule. The fact that photoexcitation of C337 in aromatic amine solvents initiates electron transfer is in full accordance with the large body of work obtained using other coumarin dyes.[8,16] Whereas most of these studies involve time-resolved emission studies, providing information only on the forward electron transfer step, Wang et al. performed UV/vis electronic pump−probe spectroscopy of C337 in DMAN, and by monitoring the transient absorption at 500 nm, where the $DMAN^{\bullet+}$ is understood to absorb, they derived a 4 ps time constant for the forward electron transfer reaction.[11] Wang et al. did not discuss the back electron reaction of the charge-separated species. We also performed femtosecond UV/vis pump−probe spectroscopy of C337 in DMAN. A straightforward interpretation appears to be impossible due to strong overlap of the absorption of $DMAN^{\bullet+}$ with the stimulated emission of C337 at early pulse delays (see Supporting Information, Figures S1 and S2), which may be affected by solvation dynamics as well. Measurement of the transient IR response of the C≡N stretching vibration of $C337^{\bullet-}$ appears to lead to results that are easier to interpret. Whereas Wang et al. do not report on the ET dynamics

dx.doi.org/10.1021/jp108090b |J. Phys. Chem. A 2011, 115, 664–670

that can be derived from the time-dependent absorption of the C≡N stretching marker mode, we have derived both forward and backward ET reaction time scales in all solvents. We note that the small additional 14 cm^{-1} red-shift of the C≡N stretching vibration, when C337 in the S_1-state converts to $C337^{\bullet-}$, indicates that the additional electron density in $C337^{\bullet-}$ is located in an orbital with antibonding character along the C≡N bond, but that a larger effect on the C≡N bond is obtained when promoting an electron in C337 from the HOMO to the LUMO by photoexcitation.

We do not observe a large solvent dependence in forward ET transfer rates, when comparing the experimental kinetics traces obtained in DMAN, MAN, and AN. As a result, there is no direct connection between a pronounced red-shift in C═O stretching vibration, i.e., the formation of a hydrogen bond between the C═O group of C337 and a solvent molecule, and the forward ET process. In addition to that, the absence of a pronounced isotope effect in the forward and backward ET steps in AN strongly suggests that hydrogen bonds of the solvent to the solute, or between solvent molecules, are not playing a key role in mediating ET between C337 and the electron donating aromatic amine solvent molecules. Instead, other factors, such as solvation dynamics of the polar solvent or differences in electronic coupling coefficients, are likely more important in dictating ET rates. Similar conclusions were drawn in the reports by Yoshihara and co-workers.[8]

We now calculate the free energy changes (ΔG_0) for the forward ET reactions of photoexcited C-337 and anilines. The free energy changes (ΔG_0) for the ET reactions between the ground state anilines (donors) and the excited state C-337 (acceptor) in neat aniline solvent can be expressed as[17]

$$\Delta G_{CSET}{}^{o} = E(D/D^{+}) - E(A/A^{-}) - E_{00} - \frac{e^2}{\varepsilon r_{DA}} \qquad (1)$$

where E_{00} is the 0−0 transition energy (between the S_0 and S_1 states) of the C337, $E(A/A^{-})$ is the reduction potential of C337, $E(D/D^{+})$ is the oxidation potential of neat anilines, and $e^2/\varepsilon r_{DA}$ is the stabilization energy of the product ion pair state in anilines (where e is the charge of an electron, ε is the dielectric constant of the solvent, and r_{DA} is the distance between donor−acceptor pair). Using eq 1 we have determined $\Delta G_{CSET}{}^{o}$ to be −0.55 eV for AN, −0.67 eV for MAN, and −0.72 eV for DMAN. Considering Marcus ET theory,[18] we expect faster ET reaction rates when going from AN, via MAN, to DMAN. Based on the fact that the influence of hydrogen bonds seems to be absent, and the fact that the ET driving force does not govern the ET rates, all the donor−acceptor pairs have special−and similar−interactions dominating the ET dynamics, which allows them to react with similar reaction rates.

From Shirota et al. we learn that the early time component of solvation dynamics in DMAN is about two times slower than in MAN and about three times slower than in AN, whereas the long time components are similar.[8] For DMAN the solvation correlation function can be fitted with biexponential decay with time constants of $\tau_{solv,1}$ = 3.8 ps (46%) and $\tau_{solv,2}$ = 15.0 ps (54%). For MAN these constants are $\tau_{solv,1}$ = 2.0 ps (25%) and $\tau_{solv,2}$ = 16.2 ps (75%) and for AN $\tau_{solv,1}$ = 1.2 ps (28%) and $\tau_{solv,2}$ = 17.8 ps (72%). One may anticipate a direct interplay between the rearranging solvation shells and the forward ET coordinate, as solvation dynamics and forward ET occur on similar time scales. However, we do not observe any change in dynamics for forward ET in the three aromatic amine solvents. This suggests that the coupling between the solvation shells and the ET reaction coordinate remains moderate.

Di Labio and Johnson[19] have shown that $\pi-\pi$ interactions play a major role in proton-coupled electron transfer reactions. Recently Takai et al.[20] demonstrated enhanced electron transfer properties of cofacial porphyrin dimers through $\pi-\pi$ interactions. In the present investigation also we suggest that electronic interactions between the π-orbitals of C337 and the aromatic amine solvent molecules play a key role. With this we can interpret the nonexponential behavior of the forward ET reaction as being indicative of a distribution of configurations with different spatial orientations of C337 and the solvent molecules. The fastest component of 0.5 ps may be caused by those configurations where the π-orbital overlap between C337 and the aromatic amine solvent is optimal, whereas for the slower 7 ps component couplings may be smaller due to less favorable relative orientations. We can assume that once ET has occurred the $C337^{\bullet-}$ radical anion and the $DMAN^{\bullet+}/MAN^{\bullet+}/AN^{\bullet+}$ radical cation remain as an ion pair in solution, because ion pair separation does not occur in the aromatic amine solvents that have only moderate values for the dielectric constant. As a result the fate of the ion pair is to convert back to the ground state by backward ET.

In contrast we do observe a solvent dependence in backward ET rates, with, however, a less obvious order, as the fastest backward ET occurs in MAN (40 ps), followed by AN (66 ps), and the slowest backward ET is found for DMAN (110 ps). With backward ET rates much longer than solvation dynamics, we may assume that the standard Marcus theory for ET applies. Now the feasibility of backward ET reaction from reduced coumarin ($C337^{\bullet-}$) to oxidized $DMAN^{\bullet+}/MAN^{\bullet+}/AN^{\bullet+}$ is dictated by the standard free energy change ($-\Delta G^{o}$) for the ET reaction following Marcus theory. The free energy change for the backward ET reaction can be expressed as[17]

$$\Delta G_{CRET}{}^{o} = -E(D/D^{+}) + E(A/A^{-}) + \frac{e^2}{\varepsilon r_{DA}} \qquad (2)$$

Following eq 2 the calculated value of free energy change for DMAN is $\Delta G_{CRET}{}^{o}$ = −1.97 eV, for MAN it is $\Delta G_{CRET}{}^{o}$ = −2.02 eV, and for AN it is $\Delta G_{CRET}{}^{o}$ = −2.14 eV. Considering the fact that a similar type of interaction between donor−acceptor pairs occurs in all solvents studied here, we can assume that the coupling matrix elements for the backward ET reaction are similar for all three cases. Following Marcus ET theory, this estimation of the driving force for ET suggests that the back ET reaction for all the donor−acceptor pairs falls in the inverted regime of ET reactions. We can clearly observe that back ET in MAN is faster (40 ps) than in AN (66 ps), which follows Marcus ET theory. On the other hand, we expect the back ET reaction rate in DMAN to be the fastest of all three solvent cases. Instead, we observe the slowest reaction time (110 ps) in C337/DMAN. We suggest that the magnitudes of the $\pi-\pi$ interactions, which dictate the electronic couplings between donor and acceptor, may be affected by steric hindrance factors, where the geometric arrangement of the two methyl groups in DMAN might be the reason for slowing down the BET reaction in DMAN.

5. CONCLUSION

We have investigated forward and backward electron transfer (ET) dynamics between coumarin 337 (C337) (acceptor) and

the aromatic amine solvents (donor) aniline (AN), *N*-methylaniline (MAN), and *N*,*N*-dimethylaniline (DMAN) with the help of femtosecond infrared spectroscopy. Monitoring the C=O stretching vibration of C337 in the S_0-state reveals that a hydrogen bond between C337 and a solvent molecule occurs in AN and MAN. Electron transfer from amine solvents to photoexcited C337 can be deduced from the appearance of the C≡N stretching vibration band at 2166 cm^{-1} of C337 radical anion radical in the transient IR spectrum. Forward ET dynamics is found to be biexponential with time constants τ_{ET}^{1} = 500 fs, τ_{ET}^{2} = 7 ps in all solvents. This shows that hydrogen bonds between C337 and the amine solvents do not play a major role in the forward ET dynamics, which is in addition supported by the absence of an H/D isotope effect on this ET reaction step in AN. Due to the fact that driving forces for the forward ET reaction are significantly different in AN, MAN, and DMAN, we suggest that electronic interactions between the π-orbitals of C337 and the aromatic amine solvent molecules play a key role in this process. We have also followed the back ET dynamics by monitoring the transient decay of anion radical marker mode (2166 cm^{-1}) of C337 and found this reaction step to be solvent dependent. Standard Marcus theory again fails to predict the right correlation between driving force and reaction rate in the backward ET step. We suggest that steric hindrance of the dimethylamino group in the C337/DMAN may be a reason for this.

■ ASSOCIATED CONTENT

Supporting Information. Transient UV/vis absorption spectra of C337 in ACN and in DMAN measured in the visible region at different time delays after exciting C337 at 400 nm (Figure S1) and associated kinetic traces (Figure S2). Time-resolved emission kinetics of C337 in acetonitrile after excitation at 400 nm and detection at 490 nm (Figure S3). This material is available free of charge via the Internet at http://pubs.acs.org.

■ AUTHOR INFORMATION

Corresponding Author

*H.N.G.: e-mail hnghosh@barc.gov.in; fax 00-91-22-25505151. E.T.J.N.: e-mail nibberin@mbi-berlin.de..

■ REFERENCES

(1) (a) Marcus, R. A. *J. Chem. Phys.* **1956,** *24*, 966. (b) Marcus, R. A. *J. Chem. Phys.* **1956,** *24*, 979. (c) Marcus, R. A. *Annu. Rev. Phys. Chem.* **1964,** *15*, 155. (d) Barbara, P. F.; Jarzeba, W. *Adv. Photochem.* **1990,** *15*, 1. (e) Weaver, M. J.; McManis, G. E., III. *Acc. Chem. Res.* **1990,** *23*, 294. (f) *Electron Transfer in Inorganic, Organic and Biological Systems*; Bolton, J. R., Mataga, N., McLendon, G. L., Eds.; American Chemical Society: Washington, DC, 1991.(g) Newton, M. D.; Sutin, N. *Annu. Rev. Phys. Chem.* **1984,** *35*, 437. (h) Yoshihara, K.; Tominaga, K.; Nagasawa, Y. *Bull. Chem. Soc. Jpn.* **1995,** *68*, 696. (i) Zusman, L. D. *Chem. Phys.* **1980,** *49*, 295. (j) Zusman, L. D. *Chem. Phys.* **1988,** *119*, 51. (k) Rips, I.; Jortner, J. *J. Chem. Phys.* **1987,** *87*, 2090. (l) Jortner, J.; Bixon, M. *J. Chem. Phys.* **1988,** *88*, 167. (m) Gao, Y. Q.; Marcus, R. A. *J. Chem. Phys.* **2000,** *113*, 6351. (n) Marcus, R. A. *J. Electroanal. Chem.* **1997,** *438*, 251.

(2) (a) Gust, D.; Moore, T. A.; Moore, A. L. *Acc. Chem. Res.* **2001,** *34*, 40–48. (b) Barbara, P. F.; Meyer, T. J.; Ratner, M. A. *J. Phys. Chem.* **1996,** *100*, 13148–13168. (c) Hagfeldt, A.; Grätzel, M. *Chem. Rev.* **1995,** *95*, 49–68. (d) Bard, A. J.; Fox, M. A. *Acc. Chem. Res.* **1995,** *28*, 141–145. (e) Paddon-Row, M. N. *Acc. Chem. Res.* **1994,** *27*, 18–25. (f) Wasielewsky, M. R. *Chem. Rev.* **1992,** *92*, 435–461. (g) Baranoff, E.; Collin, J.-P.; Flamigni, L.; Sauvage, J.-P. *Chem. Soc. Rev.* **2004,** *33*, 147–155. (h) Collin, J.-P.; Gaviña, P.; Heitz, V.; Sauvage, J.-P. *Eur. J. Inorg. Chem.* **1998,** 1–14. (i) Sauvage, J.-P.; Collin, J.-P.; Chambron, J.-C.; Guillerez, S.; Coudret, C.; Balzani, V.; Barigelletti, F.; De Cola, L.; Flamigni, L. *Chem. Rev.* **1994,** *94*, 993–1019. (j) Imahori, H.; Norieda, H.; Yamada, H.; Nishimura, Y.; Yamazaki, I.; Sakata, Y.; Fukuzumi, S. *J. Am. Chem. Soc.* **2001,** *123*, 100–110. (k) Hagfeldt, A.; Grätzel, M. *Acc. Chem. Res.* **2000,** *33*, 269–277. (l) Bignozzi, C. A.; Argazzi, R.; Indelli, M. T.; Scandola, F. *Sol. Energy Mater. Sol.Cells* **1994,** *32*, 229–244. (m) O'Regan, B.; Grätzel, M. *Nature* **1991,** *353*, 737–740.

(3) (a) Krauss, N. *Curr. Opin. Chem. Biol.* **2003,** *7*, 540–550. Willner, I.; Willner, B. *Coord. Chem. Rev.* **2003,** *245*, 139–151. (b) Lubitz, W.; Lendzian, F.; Bittl, R. *Acc. Chem. Res.* **2002,** *35*, 313–320.

(4) (a) Piotrowiak, P. *Chem. Soc. Rev.* **1999,** *28*, 143. (b) Ward, M. D. *Chem. Soc. Rev.* **1997,** *26*, 365.(c) Sessler, J. L.; Wang, B.; Springs, S. L.; Brown, C. T. In *Comprehensive Supramolecular Chemistry*; Atwood, J. L., Davies, J. E. D., MacNicol, D. D., Vogtle, F., Murakami, Y., Eds.; Pergamon: Oxford, 1996; Vol. 4, p 311.(d) Deng, Y.; Roberts, J. A.; Peng, S.-M.; Chang, C. K.; Nocera, D. G. *Angew. Chem., Int. Ed. Engl.* **1997,** *36*, 2124. (e) Kirby, J. P.; Roberts, J. A.; Nocera, D. G. *J. Am. Chem. Soc.* **1997,** *119*, 9230. (f) Hayashi, T.; Miyahara, T.; Kumazaki, S.; Ogoshi, H.; Yoshihara, K. *Angew. Chem., Int. Ed. Engl.* **1996,** *35*, 1964. (g) Damrauer, N. H.; Hodgkiss, J. M.; Rosenthal, J.; Nocera, D. G. *J. Phys. Chem. B* **2004,** *108*, 6315. (h) Hodgkiss, J. M.; Damrauer, N. H.; Pressé, S.; Rosenthal, J.; Nocera, D. G. *J. Phys. Chem. B* **2006,** *110*, 18853. (i) Reece, S. Y.; Nocera, D. G *Annu. Rev. Biochem.* **2009,** *78*, 673.

(5) Cooley, L. F.; Headford, C. F. L.; Elliott, C. M.; Kelly, D. F. *J. Am. Chem. Soc.* **1988,** *110*, 6673.

(6) (a) Bowler, B. E.; Meade, T. J.; Mayo, S. L.; Richards, J. H.; Gray, H. B. *J. Am. Chem. Soc.* **1989,** *111*, 8757. (b) Therien, M. J.; Selman, M.; Gray, H. B.; Chang, I.-J.; Winkler, J. R. *J. Am. Chem. Soc.* **1990,** *112*, 2420. (c) Beratan, D. N.; Betts, J. N.; Onuchic, J. N. *Science* **1991,** *252*, 1285. (d) Philip, D.; Stoddart, J. F. *Angew. Chem., Int. Ed. Engl.* **1996,** *35*, 1154.

(7) (a) de Rege, P. J. F.; Williams, S. A.; Therien, M. J. *Science* **1995,** *269*, 1409–1413. (b) Turro, C.; Chang, C. K.; Leroi, G. E.; Cukier, R. I.; Nocera, D. G. *J. Am. Chem. Soc.* **1992,** *114*, 4013–4015. (c) Kirby, J. P.; Roberts, J. A.; Nocera, D. G. *J. Am. Chem. Soc.* **1997,** *119*, 9230–9236. (d) Roberts, J. A.; Kirby, J. P.; Wall, S. T.; Nocera, D. G. *Inorg. Chim. Acta* **1997,** *263*, 395–405. (e) Williamson, D. A.; Bowler, B. E. *J. Am. Chem. Soc.* **1998,** *120*, 10902–10911.

(8) (a) Nagasawa, Y.; Arkadiy, T.; Yartsev, P.; Tominaga, K.; Bisht, P. B.; Johnson, A. E.; Yoshihara, K. *J. Phys. Chem.* **1995,** *99*, 653–662. (b) Nagasawa, Y.; Arkadiy, T.; Yartsev, P.; Tominaga, K.; Johnson, A. E.; Yoshihara *J. Am. Chem. Soc.* **1993,** *115*, 7922–7923. (c) Pal, H.; Nagasawa, Y.; Tominaga, K.; Yoshihara, K. *J. Phys. Chem.* **1996,** *100*, 11964–11974. (d) Shirota, H.; Pal, H.; Tominaga, K.; Yoshihara, K. *J. Phys. Chem. A* **1998,** *102*, 3089–3102. (e) Rubtsov, I. V.; Shirota, H.; Yoshihara, K. *J. Phys. Chem. A* **1999,** *103*, 1801–1808. (f) Shirota, H.; Pal, H.; Tominaga, K.; Yoshihara, K. *J. Phys. Chem. A* **1998,** *102*, 3089–3102.

(9) (a) Singh, A. K.; Mondal, J. A.; Ramakrishna, G.; Ghosh, H. N.; Bandyopadhyay, T.; Palit, D. K. *J. Phys. Chem. A* **2005,** *109*, 4014–4023. (b) Glusac, K.; Goun, A.; Fayer, M. D. *J. Chem, Phys* **2006,** *125*, 054712.

(10) (a) Mohammed, O. F.; Banerji, N.; Lang, B.; Nibbering, E. T. J.; Vauthey, E. *J. Phys. Chem. A* **2006,** *110*, 13676–13680. (b) Mohammed, O. F.; Adamczyk, K.; Banerji, N.; Dreyer, J.; Lang, B.; Nibbering, E. T. J.; Vauthey, E. *Angew. Chem., Int. Ed.* **2008,** *47*, 9044–9048.

(11) Wang, C.; Akhremitchev, B.; Walker, G. C. *J. Phys. Chem. A* **1997,** *101*, 2735.

(12) (a) Chudoba, C.; Nibbering, E. T. J.; Elsaesser, T. *Phys. Rev. Lett.* **1998,** *81*, 3010. Chudoba, C.; Nibbering, E. T. J.; Elsaesser, T. *J. Phys. Chem. A* **1999,** *103*, 5625. (b) Nibbering, E. T. J.; Tschirschwitz, F.; Chudoba, C.; Elsaesser, T. *J. Phys. Chem. A* **2000,** *104*, 4236.

(13) Palit, D. K.; Zhang, T.; Kumazaki, S.; Yoshihara, K. *J. Phys. Chem. A* **2003,** *107*, 10798–10804.

(14) Liu, Y.; Ding, J.; Shi, D.; Sun, J. *J. Phys. Chem. A* **2008,** *112*, 6244–6248.

(15) Kaindl, R. A.; Wurm, M.; Reimann, K.; Hamm, P.; Weiner, A. M.; Woerner, M. J. *Opt. Soc. Am.* **2000,** *B 17*, 2086.

(16) (a) Shannon, C. F.; Eads, D. D. *J. Chem. Phys.* **1995,** *103*, 5201. (b) Castner, E. W.; Kennedy, D., Jr.; Cave, R. J. *J. Phys. Chem. A* **2000,** *104*, 2869–2885.
(17) Rehm, D.; Weller, A. *Isr. J. Chem.* **1970,** *8*, 259.
(18) Marcus, R. A.; Sutin, N. *Biochim. Biophys. Acta* **1985,** *811*, 265.
(19) Di Labio, G. A.; Johnson, E. R. *J. Am. Chem. Soc.* **2007,** *129*, 6199–6203.
(20) Takai, A.; Gros, C.; Barbe, J.-M.; Guilard, R.; Fukuzumi, S. *Chem.—Eur. J.* **2009,** *15*, 3110–3122.